Exact and Auditable LLM-Assisted Inverse Problems in Scattering Amplitudes

Constraints, Diagnostics, and Proof

Yaobo Zhang / 张曜勃
Ningxia University
Quantum Computing and Machine Learning Workshop 2026
Sun Yat-sen University (Shenzhen Campus) --- 17 August 2026

Outline

SECTION 01

Scattering amplitudes

Compact formulas, cuts, recursion, algebra, and scattering equations.

Amplitudes set scattering rates

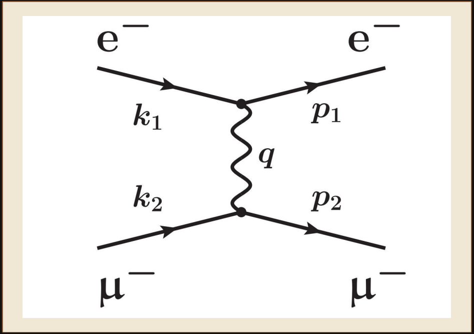

S-MATRIX ELEMENT

$$S = \mathbf{1} + i(2\pi)^D \delta^{(D)}\left(\sum_i k_i\right) \mathcal{A}_n.$$

$$d\sigma \;\propto\; \left|\mathcal{A}_n\right|^2 d\Phi_n.$$

For fixed external states, $\mathcal{A}_n$ contains the dynamics that sets cross sections and event distributions.

D. A. Kosower et al., SAGEX Review on Scattering Amplitudes, arXiv:2203.13012.

MHV compresses many diagrams to one formula

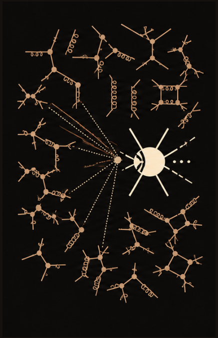

1986 / COLOR-ORDERED TREE GLUONS

$$\mathcal{A}_n^{\mathrm{MHV}} = i\,\frac{\langle ij\rangle^4}{\langle 12\rangle\langle 23\rangle\cdots\langle n1\rangle}.$$

Two negative-helicity gluons give one cyclic spinor expression.

S. J. Parke and T. R. Taylor, Phys. Rev. Lett. 56, 2459 (1986); F. A. Berends and W. T. Giele, Nucl. Phys. B 306, 759 (1988).

Unitarity cuts loops into on-shell trees

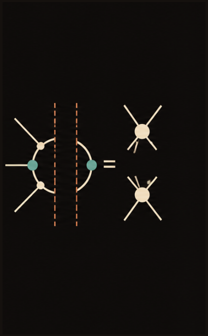

1960 / 1994

$$\mathrm{Disc}\,\mathcal{A}^{1\text{-loop}} \sim \sum_{\text{states}} \mathcal{A}_L^{\text{tree}}\,\mathcal{A}_R^{\text{tree}}\,.$$

Putting the cut propagators on shell splits a loop into products of tree amplitudes.

R. E. Cutkosky, J. Math. Phys. 1, 429 (1960); Z. Bern, L. Dixon, D. Dunbar and D. Kosower, Nucl. Phys. B 425, 217 (1994).

BCFW builds trees from factorization poles

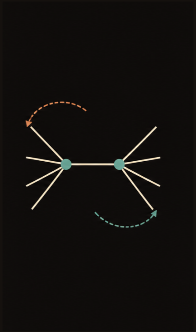

2004--05 / TREE RECURSION

$$\mathcal{A}_n(0) = \sum_{P,h} \mathcal{A}_L(z_P)\,\frac{1}{P^2}\,\mathcal{A}_R(z_P).$$

A complex shift exposes factorization poles;

their residues are lower-point on-shell amplitudes.

R. Britto, F. Cachazo and B. Feng, Nucl. Phys. B 715, 499 (2005); R. Britto, F. Cachazo, B. Feng and E. Witten, Phys. Rev. Lett. 94, 181602 (2005).

BCJ gives color and kinematics the same algebra

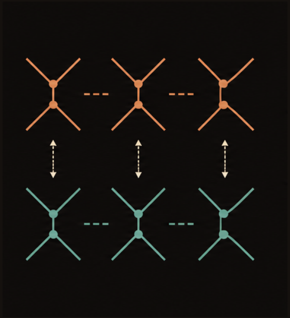

2008 / COLOR--KINEMATICS DUALITY

$$c_i + c_j + c_k = 0, \qquad n_i + n_j + n_k = 0.$$

A numerator representation can satisfy the same Jacobi relation as color.

Z. Bern, J. J. M. Carrasco and H. Johansson, Phys. Rev. D 78, 085011 (2008).

CHY puts scattering on a punctured sphere

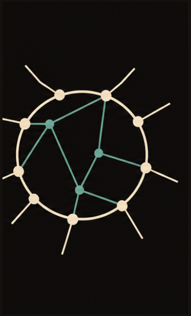

2013--15 / SCATTERING EQUATIONS

$$E_a = \sum_{b\neq a} \frac{s_{ab}}{z_a - z_b} = 0, \qquad \mathcal{A}_n = \int d\mu_n^{\mathrm{CHY}}\, I(z).$$

The scattering equations fix the punctures algebraically; graph edges encode factors of $I(z)$.

F. Cachazo, S. He and E. Y. Yuan, Phys. Rev. Lett. 113, 171601 (2014); C. Baadsgaard et al., JHEP 09 (2015) 129.

Three structures pose three inverse questions

METHOD	GIVEN	INVERSE QUESTION
CHY	required and forbidden poles	Which graph integrand realizes them?
BCJ	Jacobi identities and generalized cuts	Which numerator satisfies all data?
MHV + Lean	symmetry, boundaries, and factorization	Do the constraints leave one physical line?

S. Li and Y. Zhang, Phys. Rev. D 113, 105006 (2026); L. Mai and Y. Zhang, arXiv:2607.13412, 2608.11792.

SECTION 02

CHY and discrete backpropagation

Pole constraints become a finite exact search.

Prescribed poles define a finite exact search

INTEGER GRAPH VARIABLES

$$I(z) = \prod_{i<j} z_{ij}^{-m_{ij}}, \qquad m_{ij} \in \mathbb{Z}_{\geq 0}.$$

Each exponent is an edge multiplicity in the CHY graph.

FINITE REPRESENTATION

$$m = (m_{12}, \ldots, m_{n-1,n}) \in \mathbb{Z}_{\geq 0}^{\binom{n}{2}}.$$

Degree and pole conditions become linear equalities and inequalities in m.

C. Baadsgaard et al., JHEP 09 (2015) 129; S. Li and Y. Zhang, Phys. Rev. D 113, 105006 (2026).

Generalized pole degree tests each channel

$$K(A) = \sum_{\substack{i<j \\ i,j\in A}} m_{ij}, \qquad \chi(A) = K(A) - 2(|A| - 1)$$

REQUIRED SIMPLE POLE

$$\chi(A) = 0$$

FORBIDDEN POLE

$$\chi(A) \leq -1$$

S. Li and Y. Zhang, Phys. Rev. D 113, 105006 (2026).

Pole constraints compile to integer equations

required poles → pair data K_{ij} → subset recursion → integer system → **exact integrand**

The search variables, constraints, and output are all discrete and exact.

S. Li and Y. Zhang, Phys. Rev. D 113, 105006 (2026).

Face recursion gives the integer system

FACE RECURSION

$$K(A) = \frac{1}{|A| - 2} \sum_{\substack{B \subset A \\ |B| = |A| - 1}} K(B)$$

Repeated recursion expresses every higher-channel value in terms of pair data.

INTEGER CONSTRAINTS

$$Dm = r, \qquad B_{\text{target}} m = q, \qquad B_{\text{forbid}} m \leq q' - 1, \qquad m \in \mathbb{Z}^N$$

S. Li and Y. Zhang, Phys. Rev. D 113, 105006 (2026).

Higher-channel constraints reduce to pair data

$$K(A) = \sum_{\substack{i<j \\ i,j\in A}} K_{ij}.$$

Forward evaluation computes every subset constraint from the pair layer. **If a protected constraint changes, the residual is propagated back to free pair data.**

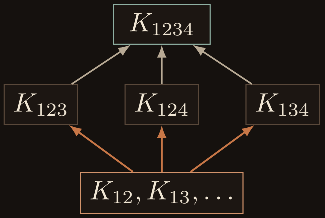

S. Li and Y. Zhang, Phys. Rev. D 113, 105006 (2026).

The six-point trace separates edit and compensation

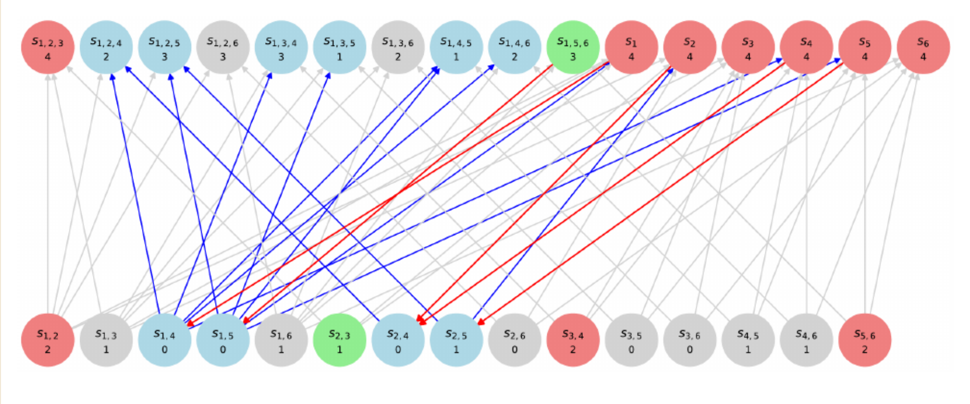

Red arrows apply the requested edit; blue arrows restore the protected constraints.

S. Li and Y. Zhang, Phys. Rev. D 113, 105006 (2026).

Backpropagation removes s_{23}

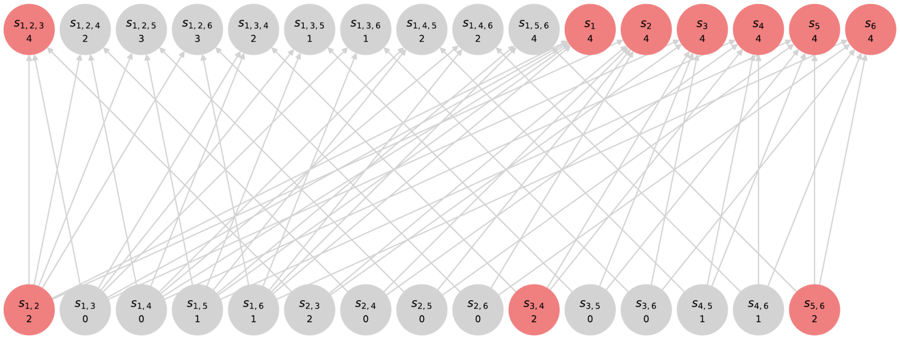

The initial network records the active channel constraints.

S. Li and Y. Zhang, Phys. Rev. D 113, 105006 (2026).

Backpropagation removes s_{23}

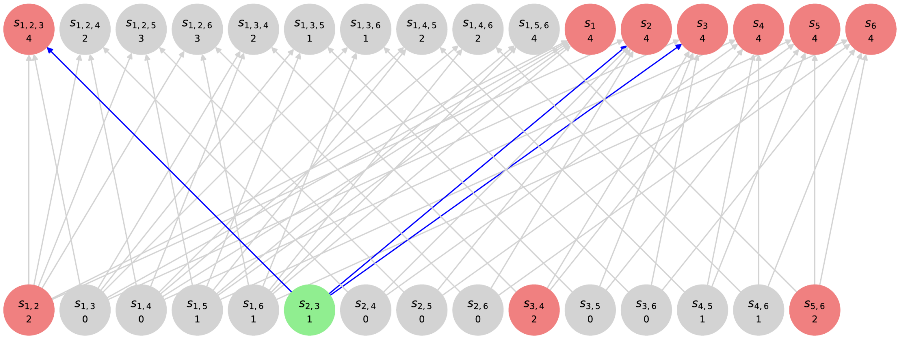

Set $\Delta K(s_{23}) = -1$ and propagate the update to its supersets.

Backpropagation removes s_{23}

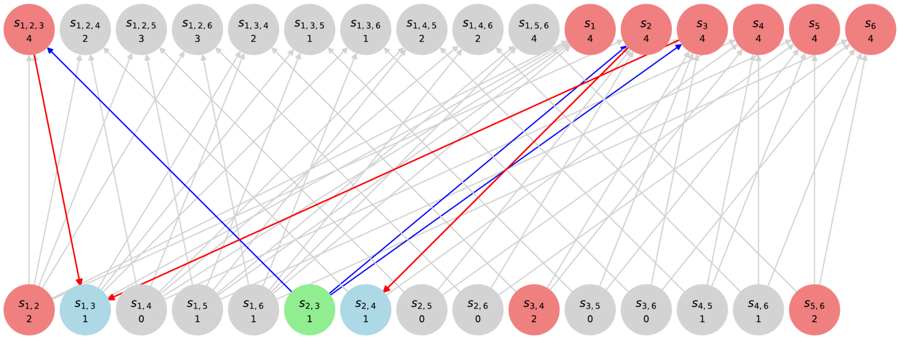

A protected node changes, so s_{13} and s_{24} are adjusted.

S. Li and Y. Zhang, Phys. Rev. D 113, 105006 (2026).

Backpropagation removes s_{23}

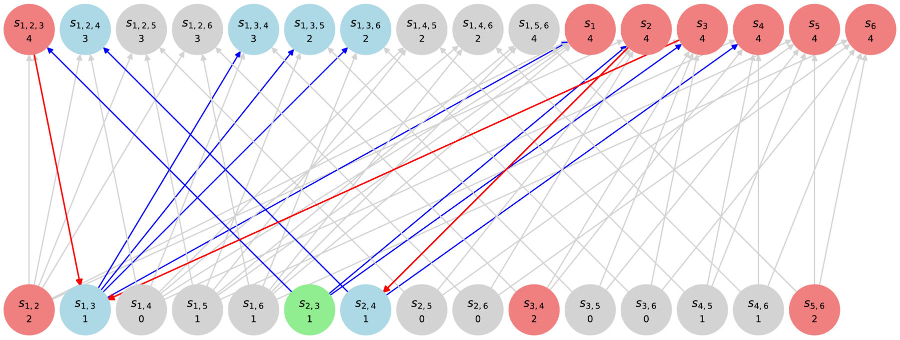

The compensating updates reach the three-particle channels.

S. Li and Y. Zhang, Phys. Rev. D 113, 105006 (2026).

Backpropagation removes s_{23}

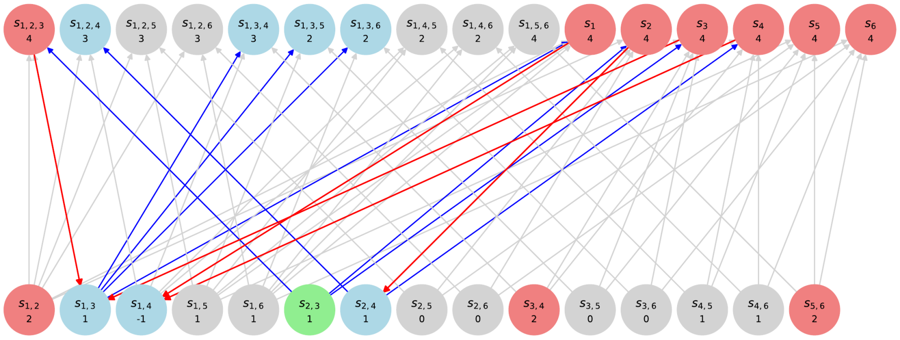

Adjust $K(s_{14})$ to satisfy the remaining recursion constraints.

S. Li and Y. Zhang, Phys. Rev. D 113, 105006 (2026).

Backpropagation removes s_{23}

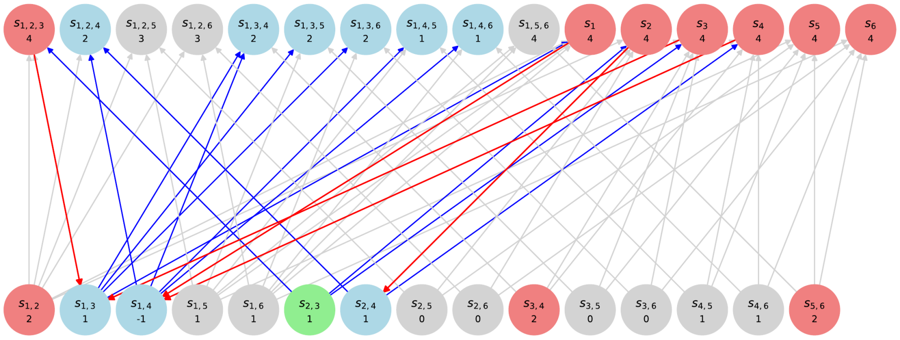

s_{23} is removed and the protected channels return to their target values.

S. Li and Y. Zhang, Phys. Rev. D 113, 105006 (2026).

Backpropagation removes s_{156}

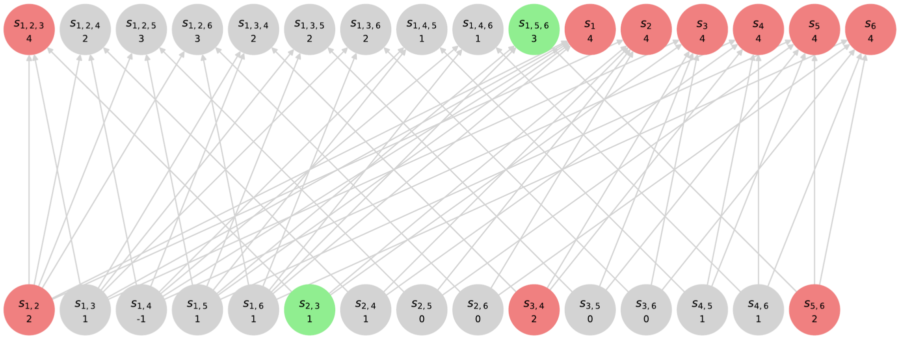

After removing s_{23}, the next target is s_{156}.

Backpropagation removes s_{156}

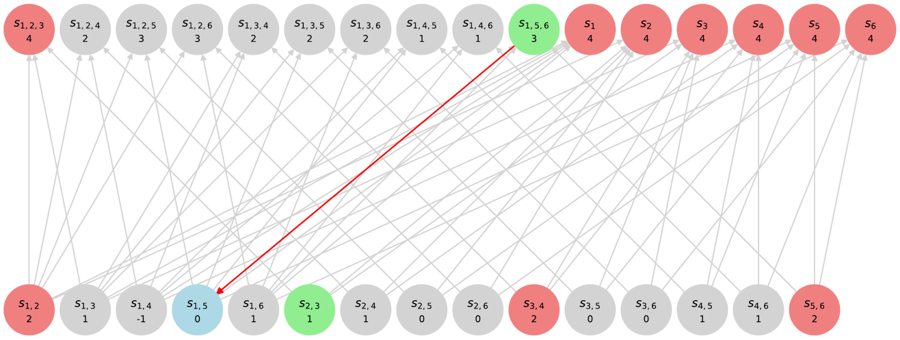

Choose the descendant s_{15} and set $\Delta K(s_{15}) = -1$.

Backpropagation removes s_{156}

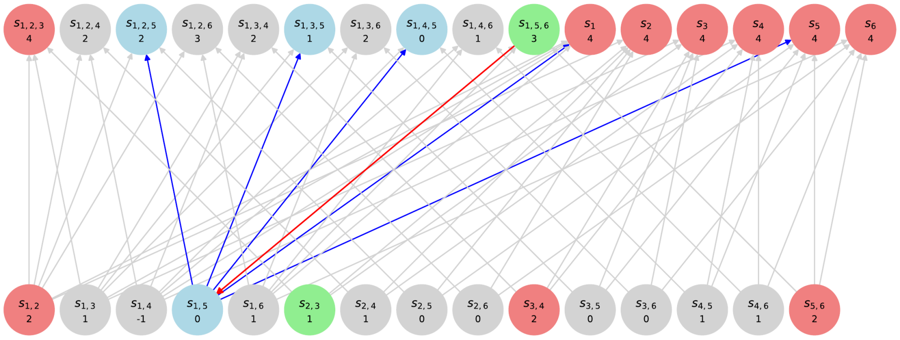

The update reaches three-particle supersets and protected nodes.

Backpropagation removes s_{156}

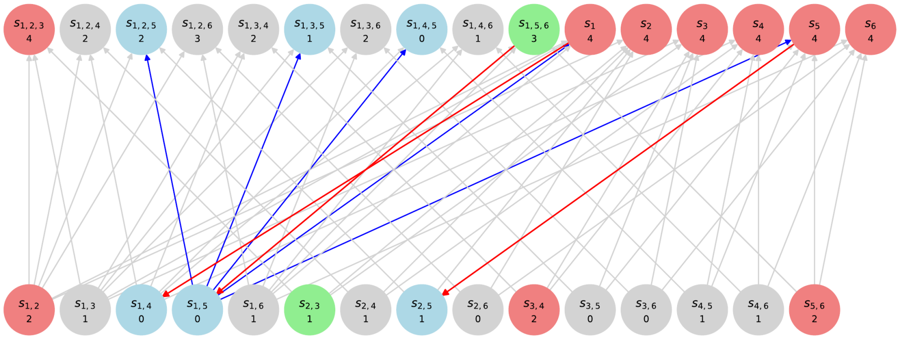

Use the free data s_{14} and s_{25} to cancel the residual.

S. Li and Y. Zhang, Phys. Rev. D 113, 105006 (2026).

Backpropagation removes s_{156}

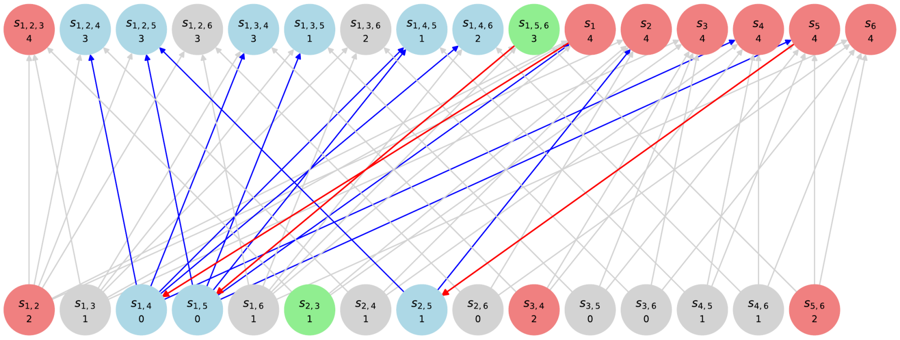

The remaining residual reaches the fixed nodes s_2 and s_4.

S. Li and Y. Zhang, Phys. Rev. D 113, 105006 (2026).

Backpropagation removes s_{156}

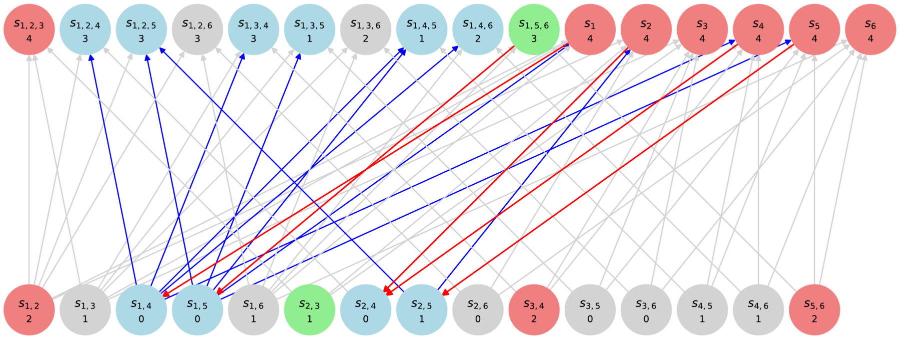

Lower $K(s_{24})$ by one to cancel the final residual.

Backpropagation removes s_{156}

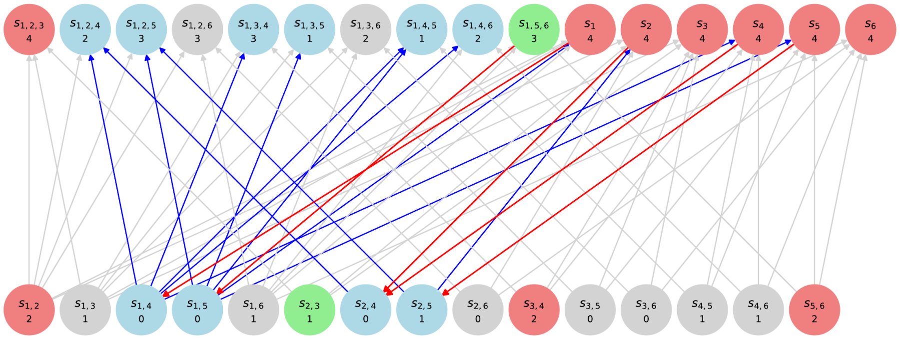

s_{23} and s_{156} are absent, with all protected channels restored.

The final integrand has the prescribed poles

INTEGRAND

$$I_6^\star = \frac{1}{z_{12}^2 z_{13} z_{16} z_{23} z_{25} z_{34}^2 z_{45} z_{46} z_{56}^2}$$

AMPLITUDE

$$\mathcal{A}_6^\star = \frac{1}{s_{12}s_{34}s_{56}} + \frac{1}{s_{123}s_{12}s_{56}}$$

The unwanted channels s_{23} and s_{156} are removed; the protected channels are unchanged.

S. Li and Y. Zhang, Phys. Rev. D 113, 105006 (2026).

SECTION 03

BCJ and the exact harness

Kernel and cokernel diagnostics determine the next revision.

BCJ cut constraints form a linear inverse problem

COMPILED SYSTEM

$$A_\sigma x = b_\sigma.$$

- x: coefficients of the numerator ansatz;
- rows: Jacobi identities and cut data;
- columns: basis elements in the ansatz.

SOLUTION SPACE

$$A_\sigma^{-1}(b_\sigma) = x_p + \ker A_\sigma.$$

Generalized-gauge freedom

changes numerator representatives without changing the observable amplitude.

$S(x_p + v) = S(x_p)$ for $v \in \ker A_\sigma$

L. Mai and Y. Zhang, arXiv:2607.13412.

The BCJ compiler returns exact diagnostics

$$x \longrightarrow N_{\text{master}} \longrightarrow \{n_g\} \longrightarrow I_g \longrightarrow A_C x$$

$$A_C = \mathrm{Cut}_C \circ \mathrm{Prop} \circ \mathrm{Jac} \circ \mathrm{Build}$$

EXACT DIAGNOSTIC TUPLE

$$\left(\operatorname{rank} A_\sigma,\ \ker A_\sigma,\ \operatorname{coker} A_\sigma,\ [b_\sigma]_{A_\sigma},\ S(\ker A_\sigma),\ \rho_T\right).$$

L. Mai and Y. Zhang, arXiv:2607.13412.

Cokernel detects an incompatible target

$$y^{\mathsf{T}}A = 0, \qquad y^{\mathsf{T}}b \neq 0, \qquad [b]_A \neq 0 \in \operatorname{coker} A$$

MEANING **The current ansatz cannot represent the cut data.**

REVISION **Add basis columns C with $y^{\mathsf{T}}C \neq 0$.**

Kernel detects unresolved directions

$$Av = 0, \qquad A^{-1}(b) = x_p + \ker A$$

MEANING **The current measurements do not distinguish v.**

REVISION **Add rows with $Rv \neq 0$, or quotient by S.**

L. Mai and Y. Zhang, arXiv:2607.13412.

Adding constraints changes both kernel and cokernel

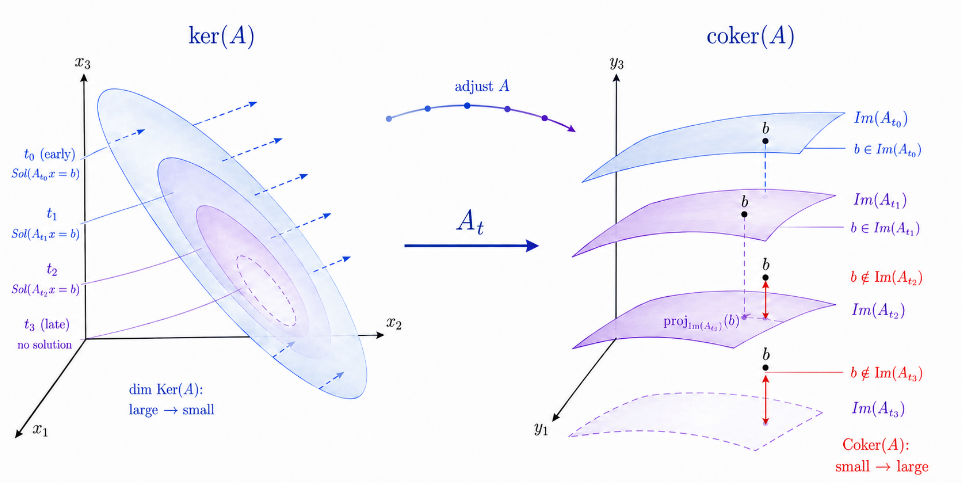

L. Mai and Y. Zhang, arXiv:2607.13412.

Held-out tests validate accepted solutions

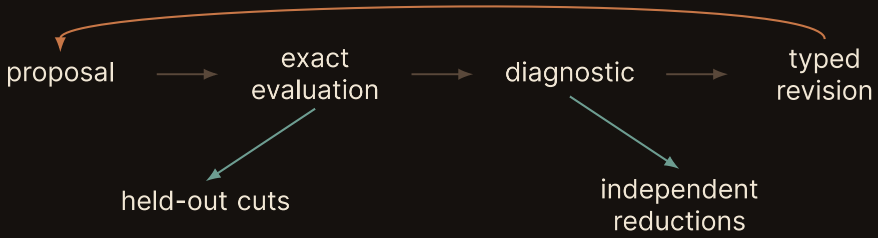

Acceptance requires fixed held-out tests.

L. Mai and Y. Zhang, arXiv:2607.13412.

Exact reduction leaves a 207-dimensional fiber

17,824 → **10,724** → **1,127**

RAW MONOMIALS → AFTER QUOTIENT → COORDINATES

$$\operatorname{rank} A = 920, \qquad \dim \ker A = 1127 - 920 = 207$$

The exact system has a 207-dimensional affine solution space.

L. Mai and Y. Zhang, arXiv:2607.13412.

The fiber has one observable image

207-dimensional solution fiber

$$\Downarrow$$

one observable class

$$S(\ker A) = 0$$

Independent reductions and helicity checks give the same observable.

L. Mai and Y. Zhang, arXiv:2607.13412.

SECTION 04

MHV and Lean

Boundary data and injectivity give a uniqueness certificate.

Symmetry reduces the MHV uniqueness test

$$\mathcal{M}_n^{\mathrm{MHV}} = \frac{N_n}{D_n}, \qquad W_n = \left(\bigcap_{i<j} J_{ij} \right)_{d(n)} = \ker \mathsf{C}_n.$$

At five and six points, pair-locus conditions give $\dim W_5 = \dim W_6 = 1$.

65,870 coordinates $\longrightarrow$ **15 exact S_7 blocks**

$$V_7 \simeq \bigoplus_{\lambda \vdash 7} S^\lambda \otimes M_\lambda, \qquad \max_\lambda \dim M_\lambda = 475$$

A. Hodges, arXiv:1204.1930; L. Mai and Y. Zhang, arXiv:2608.11792.

Seven and eight points require stronger conditions

SEVEN POINTS

$$W_{7,\mathbb{Q}} \simeq S^{(2,1^5)} \oplus S^{(1^7)}, \qquad (W_{7,\mathbb{Q}})_{\mathrm{sgn}} = \mathbb{Q}N_7^{\mathrm{Hodges}}.$$

EIGHT POINTS

$U_8 := (W_{8,\mathbb{Q}})_{\mathrm{sgn}} = \mathbb{Q}A \oplus \mathbb{Q}B,$ physical boundary data select one line.

Seven points need Bose symmetry; eight points also need boundary data.

L. Mai and Y. Zhang, arXiv:2608.11792.

Three eight-point limits select the same line

$$U_8 = \mathbb{Q}A \oplus \mathbb{Q}B, \qquad N = c_A A + c_B B.$$

$$\begin{aligned} \text{same-helicity BCFW } O(z^{-2}) &\implies 7c_A - 6c_B = 0, \\ \text{normalized } ++ \text{ collinear factorization} &\implies 7c_A - 6c_B = 0, \\ \text{normalized leading soft coefficient} &\implies 7c_A - 6c_B = 0. \end{aligned}$$

$$\ker L_{\mathrm{BCFW}} = \ker L_{\mathrm{coll}} = \ker L_{\mathrm{soft}} = \mathbb{Q}(6A + 7B)$$

All three limits fix the same coefficient ratio $7c_A = 6c_B$.

L. Mai and Y. Zhang, arXiv:2608.11792.

The all-multiplicity result has four inputs

ASSUMPTIONS

- fixed-denominator, fixed-degree alternating ansatz;
- geometric injectivity of $\rho_{ab,c}$;
- normalized $++$ factorization;
- five-point Hodges seed.

LINEAR-ALGEBRA CONSEQUENCE

$$\ker \rho = 0 \quad \Longrightarrow \quad \rho^{-1}(\mathbb{Q}\rho(h)) = \mathbb{Q}h.$$

The boundary line has at most one preimage line.

L. Mai and Y. Zhang, arXiv:2608.11792.

One injective boundary determines the all-n line

$$\rho_{ab,c} : V^{\mathrm{alt}}_{n,\mathbb{Q}} \longrightarrow Q_{n,\mathbb{Q}}/K_{ab}(c), \qquad \ker \rho_{ab,c} = 0.$$

$$\{N : \rho_{ab,c}(N) \in L_{n,ab,c}\} = \mathbb{Q}N^{\mathrm{Hodges}}_n.$$

FIVE-POINT SEED $\longrightarrow$ **NORMALIZED BOUNDARY** $\longrightarrow$ **ARBITRARY MULTIPLICITY**

Injective boundary data determine one numerator line.

L. Mai and Y. Zhang, arXiv:2608.11792.

Lean verification has a defined scope

VERIFIED IN LEAN

- consequences of the imported seven-point hook and sign decomposition;
- equality of the three eight-point probe kernels $\mathbb{Q}(6,7)$;
- boundary normalization and injectivity $\Rightarrow$ uniqueness.

IMPORTED INPUTS

- the exact spaces W_7, U_8, and projected ranks;
- ideal reductions and geometric injectivity;
- BCFW, factorization, and soft-limit theorems.

L. Mai and Y. Zhang, arXiv:2608.11792.

SECTION 05

LLM workflow

All three use typed proposals, exact evaluation, and fixed acceptance.

The three cases use the same exact workflow

physical question → typed representation → candidate revision → exact evaluation → result or next revision

CASE	REVISION	EXACT RESULT
CHY	change integer edge data	constraint-satisfying integrand
BCJ	add columns, rows, or a quotient	cokernel or kernel diagnostic
MHV + Lean	add boundary data	uniqueness certificate

LLM proposals are evaluated by exact tools

LLM PROPOSAL LAYER

- read the current constraints and diagnostics;
- propose a typed change to the representation or tests;
- record the proposal and returned evidence.

EXACT EVALUATION LAYER

- compile the proposal into exact equations or finite data;
- return ranks, kernels, residuals, or proof terms;
- apply fixed held-out tests and the stated acceptance criteria.

The LLM proposes revisions; exact physical tests determine acceptance.

Why amplitude problems fit current LLM systems

EXPLICIT STATE

Equations, graphs, pole sets, basis elements, cut rows, and boundary maps give the calculation a readable state.

BOUNDED REVISIONS

Each proposal changes one declared object while the physical acceptance criteria remain fixed.

EXACT FEEDBACK

Solvers return feasibility, residuals, kernels, cokernel witnesses, or proof goals.

INDEPENDENT ACCEPTANCE

Fixed held-out tests and Lean checks determine whether a result is accepted.

Thanks